

## COLLINEARITY AND SPIN FREEZING

I. Vincze<sup>+,++</sup> and T. Kemény<sup>+</sup>

<sup>+</sup>Research Institute for Solid State Physics, H-1525 Budapest, P.O.B. 49, Hungary

<sup>++</sup>Solid State Physics Department, Eötvös University, Budapest, Hungary

**Abstract**—An overview will be given on recent Mössbauer and magnetization investigation of the applied field dependence of the magnetic properties of typical systems without strong magnetic anisotropy and showing the absence of magnetic saturation in high fields (including iron-rich spin glass (amorphous  $\text{Fe}_{93}\text{Zr}_7$ ), soft ferromagnets (amorphous  $\text{Fe}_{88}\text{Zr}_{12}$ ,  $\text{Fe}_{70}\text{Ni}_{20}\text{Zr}_{10}$  and  $\text{Fe}_{88}\text{B}_{12}$ ) and pure Fe). The results emphasize that shape anisotropy due to surface irregularities causes misalignment between the magnetization and the applied field in the otherwise collinear magnetic structure.

### I. INTRODUCTION

Spin freezing is manifested in the disappearance of magnetization measured at low temperatures and in low applied magnetic fields. It is observed in many systems without strong magnetic anisotropy: the transition at the spin freezing temperature  $T_f$  may take place directly from the paramagnetic state (spin glasses, SG) or from a collinear ferromagnetic structure (re-entrant spin glasses, RSG) as the temperature is decreased [1,2]. Typical systems are the AuFe alloys around 16 at.% Fe and the iron rich amorphous alloys with about 10 at.% early transition element content (Zr, Sc, Hf, Y, etc.).

Spin freezing is correlated with the absence of magnetic saturation even in large applied fields ( $\approx 15$  T) [3,4]. In general, this behaviour is attributed to the presence of antiferromagnetically coupled magnetic moments resulting in non-collinear, canted spin arrangement which is caused by competing ferromagnetic and antiferromagnetic exchange interactions.

Direct evidence of spin canting is given via Mössbauer (mostly  $^{57}\text{Fe}$ ) spectroscopy. In magnetically split spectra the relative intensity of the second and fifth lines  $I_{2,5}$  (corresponding to the  $\Delta m = 0$  nuclear transitions) is given by  $I_{2,5} = 4\sin^2\Theta/(1+\cos^2\Theta)$ , where  $\Theta$  is the angle between the magnetic moment and the magnetic field  $B_{\text{ext}}$ , applied parallel to the  $\gamma$ -beam direction which is perpendicular to the sample surface. A random Fe spin orientation corresponds to  $I_{2,5} = 2$ , while  $I_{2,5} = 0$  indicates that all the Fe magnetic moments are collinear to  $B_{\text{ext}}$ , i.e. complete saturation is achieved. Investigations performed in external fields (2-3 T) well above the demagnetization field showed non-vanishing  $I_{2,5}$  intensities indicating persistent misalignment with the applied field direction [e.g. 5,6].

It is difficult to determine the extent of the magnetic correlations: short-range, close neighbourhood contributions are probed via the transferred hyperfine fields of non magnetic impurities like  $^{197}\text{Au}$  [e.g. 7] and  $^{119}\text{Sn}$  [e.g. 8], its temperature dependence is compared to that of the magnetic atoms (e.g.  $^{57}\text{Fe}$ ). These investigations are hampered by the poor resolution of the respective Mössbauer spectra. In case of Sn further complication is caused by the extreme temperature dependence of the

neighbour site contributions, which — for example — results in a change of the sign of the tin hyperfine field not shown by the polarizing Co in CoSn [9]. However, a common feature of the results is that the spin canting does not take place on a local atomic scale though the range of the correlations are unknown.

Surprisingly, recent polarized neutron [10], Mössbauer [11, 12] and high-field magnetization [13] measurements suggest that iron based amorphous ferromagnets with added metalloids show possible non-collinear spin structure: the magnetic moments fail to align in the direction of even a 4 T magnetic field. These alloys on the other hand show many typical features of ideal soft magnetic materials and any sign of low temperature spin freezing is missing. Current magnetoresistance and Mössbauer measurements show the absence of saturation even at 5 T in granular Fe-Ag system, suggesting the existence of nonaligned Fe moments with the applied field direction [14]. The magnetization of fine ( $\approx 30$  nm) amorphous iron particles ( $\mu_{\text{Fe}} = 1.7 \mu_{\text{B}}$ ) showing soft ferromagnetic properties was also not fully saturated at 2 T [15].

These unusual observations are the subject of the present paper. Detailed comparison of spin glasses with large magnetic moment concentration and soft ferromagnets with incomplete ferromagnetic alignment of moments will provide valuable information on the mechanism causing the absence of magnetic saturation.

Magnetization and high-field Mössbauer results of a spin glass-like amorphous  $\text{Fe}_{93}\text{Zr}_7$  alloy will be compared with those of ferromagnetic counterparts: amorphous  $\text{Fe}_{88}\text{Zr}_{12}$  and  $\text{Fe}_{70}\text{Ni}_{20}\text{Zr}_{10}$ . Measurements on amorphous  $\text{Fe}_{88}\text{B}_{12}$  showing soft ferromagnetic properties and on pure Fe will also be presented.

### II. EXPERIMENTAL

The Mössbauer measurements were performed using a conventional constant acceleration spectrometer with a 50 mCi  $^{57}\text{CoRh}$  source at room temperature. The external magnetic field was applied parallel to the  $\gamma$ -beam using a 7-T Janis superconducting magnet. The magnetization was measured up to 1.9 T by a vibration sample (Foner-type) magnetometer with a resolution of  $10^{-4}$  emu.

The amorphous samples were prepared by melt spinning in vacuum. The ribbon pieces are 12  $\mu\text{m}$  thick and 0.5-1 mm wide. The amorphous state of the alloys was checked by X-ray and Mössbauer measurements.

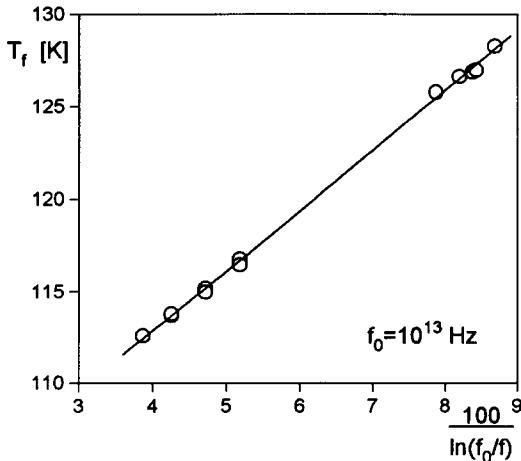


Fig. 1 Frequency dependence of the freezing temperature,  $T_f$  of amorphous  $\text{Fe}_{93}\text{Zr}_7$  taken from Ref. 16.

The magnetization of amorphous  $\text{Fe}_{93}\text{Zr}_7$  measured in 1 mT as a function of temperature exhibits the well-known cusp-type behaviour characteristic of the paramagnetic-spin glass transition at about  $T_f = 105$  K [16]. The frequency dependence of  $T_f$  shown in Fig. 1 could be well described by a Fulcher-type relation, the characteristic temperature of the interaction is  $T_0 = 100$  K. The ratio  $(T_f - T_0)/T_f$  is 0.05 for this alloy which is typical of metallic spin glasses, larger values by at least one order of magnitude are reported for systems showing the progressive freezing of clusters, i.e. an interacting superparamagnetic-like behaviour [17].

The studied amorphous  $\text{Fe}_{88}\text{Zr}_{12}$ ,  $\text{Fe}_{70}\text{Ni}_{20}\text{Zr}_{10}$  and  $\text{Fe}_{88}\text{B}_{12}$  alloys show no evidence for low temperature spin freezing, they are ferromagnetic with Curie temperatures  $T_c = 269$  K, 476 K and 502 K, respectively.

The 12  $\mu\text{m}$  thick iron foils were cold rolled from high purity bulk material in two steps, some part of it was annealed at 914 C for 2 hours in dry hydrogen to produce stress-free, recrystallized grain structure as confirmed by X-ray and Vickers-hardness measurements. The iron powder was composed of grains of  $\approx 30$   $\mu\text{m}$  diameter. As a comparison a 1  $\mu\text{m}$  thick iron layer was evaporated to a single crystal Si substrate in a  $10^{-9}$  mbar UHV system.

### III. RESULTS AND DISCUSSION

The high field susceptibility of amorphous  $\text{Fe}_{93}\text{Zr}_7$  ( $3 \text{ emu/gT}^{-1}$ ) is almost two orders of magnitude larger than that of pure Fe. Magnetic saturation was not achieved in applied fields up to 11 T [4]. Our Mössbauer results

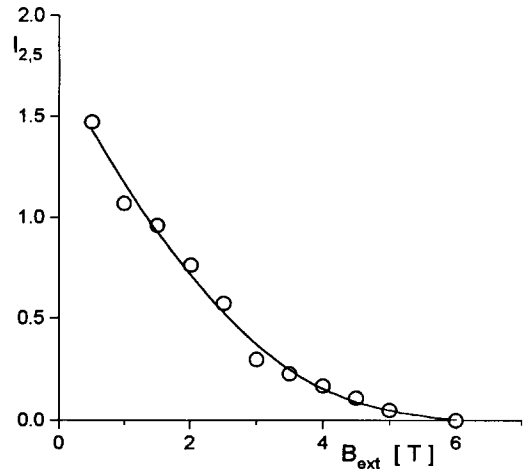


Fig. 2 External field dependence of the relative intensities of the 2-5 lines  $I_{2,5}$  at 4.2 K for amorphous  $\text{Fe}_{93}\text{Zr}_7$ .

presented in Fig. 2, on the other hand confirmed that the collinear magnetic state was reached below 6 T at 4.2 K [18]. The magnetic splitting of the Mössbauer spectra measures the absolute magnitude of the local iron magnetic moment. An increase in the average of this moment was found as a result of the applied field. The iron high field susceptibility in the collinear state was determined from the magnetic field dependence of the hyperfine fields. Its magnitude was in good agreement with the value obtained from the bulk magnetic measurements [18]. The flip of the assumed antiferromagnetically aligned iron magnetic moments with the applied field would result in a much larger increase in the bulk magnetization since according to the Mössbauer results the absolute value of the iron

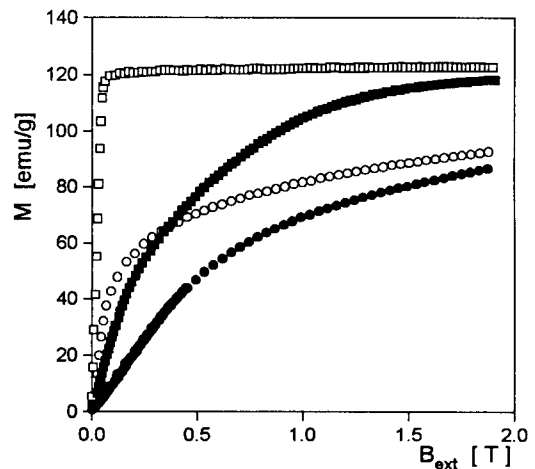


Fig. 3 Magnetization of amorphous  $\text{Fe}_{88}\text{Zr}_{12}$  (squares) and  $\text{Fe}_{93}\text{Zr}_7$  (circles) at 23 K in external fields applied parallel (empty symbols) and perpendicularly (filled symbols) to the sample surface.

magnetic moments increased. These results do not support theoretical calculations suggesting noncollinear spin structures for amorphous iron and iron based alloys [19].

In intermediate magnetic fields the low temperature magnetization curves of amorphous  $\text{Fe}_{93}\text{Zr}_7$  show some unexpected features depending on the sample geometry (Fig. 3). The curve measured in perpendicular external fields can not be transformed to the curve obtained in parallel geometry by simply taking into account the values of the demagnetization fields which in this case obviously depend on the applied field. Similar behaviour was observed in the case of ferromagnetic amorphous  $\text{Fe}_{88}\text{Zr}_{12}$  also shown in the figure. At this composition the magnetization in the parallel direction quickly increases to its saturation value. (The high field susceptibility contribution is smaller by a factor of five in this case). On the other hand, in the perpendicular geometry this saturation value is not reached in fields of 1.9 T, well above the demagnetization field of  $B_d=1.2$  T. The curved shape of the magnetization vs. field curve instead of the expected linear dependence clearly shows that it will not transform into the parallel magnetization curve.

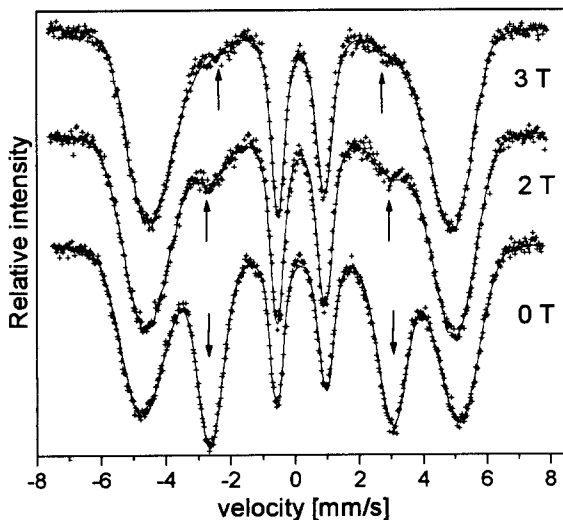


Fig. 4 Typical Mössbauer spectra of amorphous  $\text{Fe}_{88}\text{B}_{12}$  at 4.2 K in different external fields applied parallel to the  $\gamma$ -beam direction. The value of the demagnetization field in this perpendicular geometry is 1.9 T. The calculated position of the second and fifth lines are shown.

These anomalous features are remarkably similar to those observed in soft ferromagnets and granular systems mentioned in the Introduction and which were attributed to a noncollinear magnetic structure. Fig. 4 presents field dependent Mössbauer spectra of amorphous  $\text{Fe}_{88}\text{B}_{12}$  in the perpendicular geometry showing non-vanishing 2-5 line intensities in 3 T ( $B_d=1.9$  T). Similar observations were reported for amorphous  $\text{Fe}_{86}\text{B}_{14}$  and  $\text{Fe}_{80}\text{B}_{20}$  [12, 20]

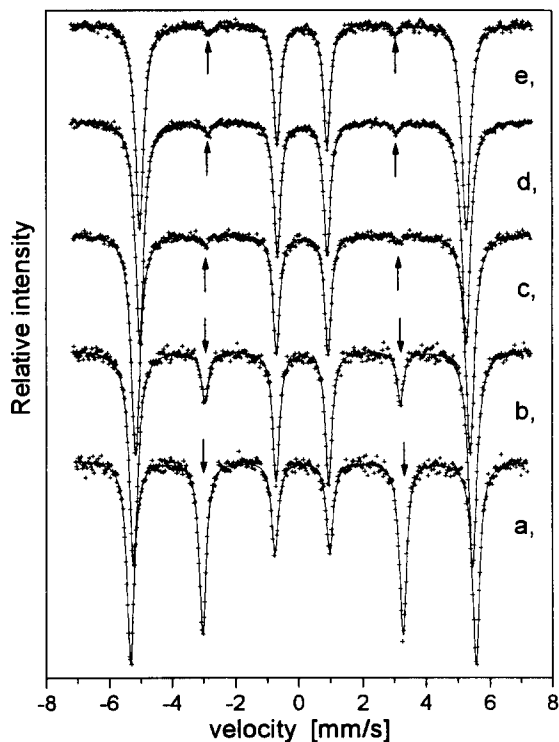


Fig. 5 Typical Mössbauer spectra of Fe at 4.2 K in different external fields applied parallel to the  $\gamma$ -beam direction. The samples are the following: 12  $\mu\text{m}$  thick cold-rolled Fe foil in  $B_{\text{ext}}=0$  T (a), 2 T (b) and 4 T (d); in 4 T the same foil annealed at 914 C for 2 hours (e); and Fe powder in 2 T (c), respectively. The calculated position of the second and fifth lines are shown.

indicating different amount of non-alignment with the applied field direction even in 5 T.

The surprising result of the present investigations is that pure Fe behaves the same manner: in the perpendicular geometry complete collinearity was not found with the applied field up to 7 T although  $B_d=2.2$  T at 4.2 K. Typical field dependent Mössbauer spectra are shown in Fig. 5, the intensities of the 2-5 lines are presented in Fig. 6. The obtained  $I_{2,5}(B_{\text{ext}})$  curves are rather similar to those reported for the magnetically soft amorphous Fe-B alloys [12, 20] and resemble for the curves of spin glass and re-entrant spin glass type alloys (Fig. 2, [18], [22]). The resolution of the pure Fe spectra is much better than those of the amorphous alloys where broad lines are observed due to the distribution of hyperfine fields. This explains why the non-vanishing  $I_{2,5}$  can be observed to much higher fields in the case of pure Fe.

Early report of the problem associated with the moment collinearity in pure Fe is found in the paper of Foner et al. [21], where the results of the first polarized Mössbauer source-absorber experiment were published. It was found

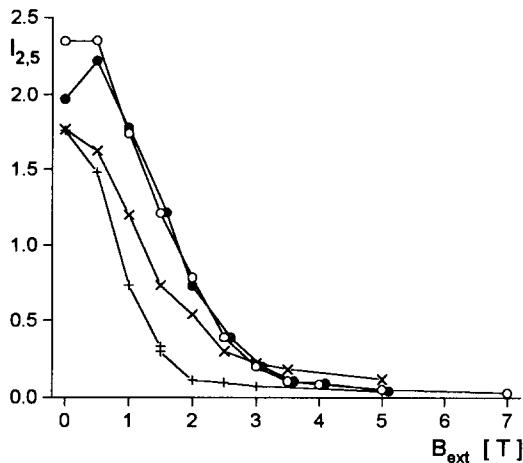


Fig. 6 External field dependence of the relative intensities of the 2-5 lines  $I_{2,5}$  at 4.2 K for 12  $\mu\text{m}$  thick cold-rolled Fe foil (dots); the same foil annealed at 914 C for 2 hours (circles); 300 nm thick Fe foil evaporated onto Al-foil (x) and Fe powder (+).

that fields of the order of 3 T applied perpendicular to the plane of the iron foil were necessary to align completely the magnetization along the external field direction. The fact that the Fe foil can only be saturated by a transversal field significantly higher than the established demagnetizing field was attributed to the anisotropy energy associated with the rotation of domains and movement of domain boundaries.

To test this assumption we have made extensive annealing tests. 914 C annealing removes the stress of the cold rolled iron foils and decreases the Vickers-hardness by about 40%. It results only in changes of  $I_{2,5}$  at low fields: its zero field value increases from 2 (characteristic of the random spin alignment) to the larger value reflecting the increased role of in-plane shape anisotropy. The rest of the  $I_{2,5}(B_{\text{ext}})$  dependencies remains unchanged for the cold rolled and annealed iron foils (Fig. 6).

It is clear that even for pure iron the spins are not parallel to the applied field above  $B_d$ . The only characteristic deviation between the  $I_{2,5}$  curves of the investigated samples is associated with their different macroscopic shape (foil, layer evaporated onto Al-foil or powder) resulting in different demagnetization field (the demagnetization factor for powder is less than for a foil). Magnetization curve of a cold rolled Fe-foil in the perpendicular geometry as a function of the external field reduced by the value of  $B_d$  shown in Fig. 7 deviates from the theoretically expected linear behaviour. The deviation in this geometry is even larger for the ferromagnetic amorphous  $\text{Fe}_{88}\text{Zr}_{12}$  in this intermediate field range.

However, if extreme precaution is taken to produce mirror-like magnetic surface as in the case of 1  $\mu\text{m}$  thick iron layer evaporated in UHV on a Si single-crystal surface the magnetization in the perpendicular geometry will

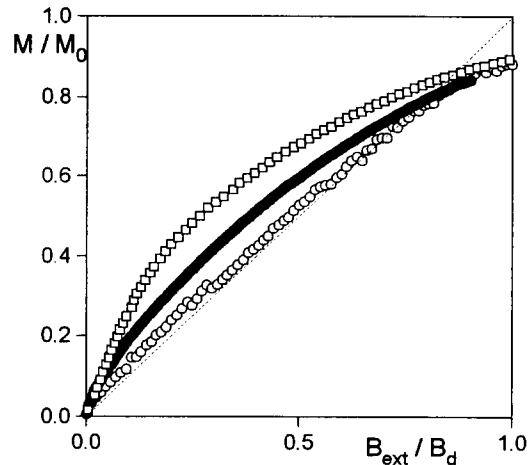


Fig. 7 Reduced magnetization vs. reduced external field at room temperature for 1  $\mu\text{m}$  thick Fe foil evaporated onto Si substrate (circles), for 12  $\mu\text{m}$  thick cold-rolled Fe foil (dots) and for amorphous  $\text{Fe}_{88}\text{Zr}_{12}$  (squares) at 23 K. The external field is perpendicular to the sample surface and normalized to the value of the demagnetization field,  $B_d$  (2.1 T for Fe and 1.2 T for  $\text{Fe}_{88}\text{Zr}_{12}$ , respectively). The value of the magnetization is normalized to the saturation value,  $M_0$  obtained in parallel geometry. The broken line marks the theoretically expected behaviour.

reproduce the theoretically expected linear field dependence as shown in Fig. 7. Small deviation from this expected behaviour was found only at the highest applied fields.

Since the foils and ribbons generally used in the measurements are far from the ideal flat surfaces and the overlapping powder particles are far from the ideal spherical shape it is really not surprising that tilting of the bulk moment from the external field direction is observed. The magnetization and the applied field is fully parallel only in rather special circumstances: in the case of ideal surfaces with well-determined orientation. It is surprising, however, that small deviations from the ideal conditions generally neglected in the experiments (waviness, surface roughness) will result in rather marked anomalies even in the absence of strong magnetic anisotropy. This observation also explains the existing discrepancies about the magnitude of noncollinearity of nominally identical systems [12, 20].

The presented results cast some doubts to the assumptions that the magnetic anomalies are caused either by antiferromagnetically aligned moments or by strong local anisotropies. Detailed composition, temperature and magnetic field dependent Mössbauer study may give some hint of the underlying mechanism. In the following the Mössbauer results on the approach to magnetic saturation will be compared in two amorphous alloys:  $\text{Fe}_{88}\text{Zr}_{12}$  and  $\text{Fe}_{70}\text{Ni}_{20}\text{Zr}_{10}$ . The increase of the Zr content results in the disappearance of the low temperature spin freezing phenomena observed in  $\text{Fe}_{93}\text{Zr}_7$ . The border composition

is  $\text{Fe}_{88}\text{Zr}_{12}$  which shows no sign of low temperature anomaly, it behaves like usual ferromagnets as shown in Fig. 3. Addition of Ni acts the same way, the low temperature magnetization anomaly of  $\text{Fe}_{90}\text{Zr}_{10}$  disappears already when 5 at. % Fe is replaced by Ni.

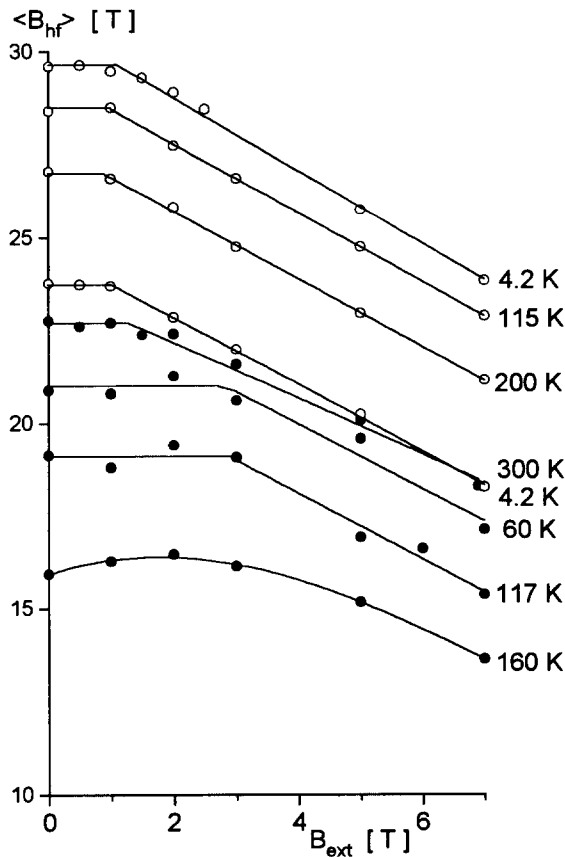


Fig. 8 External field dependence of the average hyperfine field,  $\langle B_{\text{hf}} \rangle$  as a function of temperature for amorphous  $\text{Fe}_{70}\text{Ni}_{20}\text{Zr}_{10}$  (circles) and  $\text{Fe}_{88}\text{Zr}_{12}$  (dots).

The hyperfine interaction is negative, so the hyperfine field is known to be oriented antiparallel to the magnetic moment, i.e. to the applied field in a ferromagnet. This means that above saturation (in the collinear state) the absolute value of the iron hyperfine field,  $B_{\text{hf}}$  should decrease in direct proportion to the applied field. Slower decrease of  $B_{\text{hf}}$  with  $B_{\text{ext}}$  corresponds to an induced increase in the magnetic moment of iron characterized by the value of the high field susceptibility. Below saturation the applied transversal field is compensated by the demagnetizing field, the effective field vanishes at the site of the nuclei: unchanged  $B_{\text{hf}}$  is expected as a function of  $B_{\text{ext}}$ . Exactly this behaviour is observed for amorphous  $\text{Fe}_{70}\text{Ni}_{20}\text{Zr}_{10}$  as shown in Fig. 8. At 4.2 K the barely

detectable high field susceptibility agrees well with the magnetization result [18]. The increase of temperature only shifts these curves which is characteristic for good ferromagnets.

On the other hand, the Mössbauer magnetization curves of amorphous  $\text{Fe}_{88}\text{Zr}_{12}$  do not follow this expected behaviour as a function of temperature. The results shown in Fig. 8 up to  $T/T_c \approx 0.6$  are clearly different, in a broad field range a rather strong increase in  $B_{\text{hf}}$  compensates the decrease due to  $B_{\text{ext}}$ .

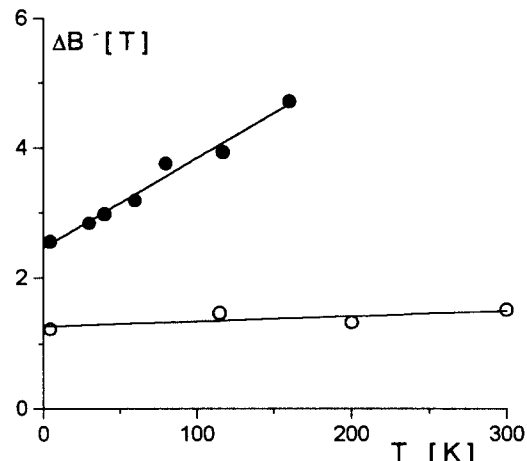


Fig. 9 Difference of  $B_{\text{plus}} = \langle B_{\text{hf}} \rangle + B_{\text{ext}}$  between 7 T and 0 T as a function of temperature for amorphous  $\text{Fe}_{70}\text{Ni}_{20}\text{Zr}_{10}$  (circles) and  $\text{Fe}_{88}\text{Zr}_{12}$  (dots).

The quantity defined as  $B_{\text{plus}} = \langle B_{\text{hf}} \rangle + B_{\text{ext}}$  cancels the decrease of  $B_{\text{hf}}$  caused by  $B_{\text{ext}}$  and it saturates with zero slope at the value  $(B_{\text{hf}} + B_{\text{d}})$  if no induced moment is present [18]. The difference  $\Delta B = B_{\text{plus}}(B_{\text{ext}} = 7\text{T}) - B_{\text{plus}}(B_{\text{ext}} = 0\text{T})$  will be given by the sum of  $B_{\text{d}}$  and the increase of hyperfine field caused by the magnetic moments induced in 7 T.  $\Delta B$  is shown for these alloys as a function of temperature in Fig. 9. It is clear that the temperature dependence of the high field susceptibility is rather different for the two investigated alloys: it is quite strong for  $\text{Fe}_{88}\text{Zr}_{12}$  and practically temperature independent for  $\text{Fe}_{70}\text{Ni}_{20}\text{Zr}_{10}$ .

The temperature dependence of the individual magnetic moments is determined by their exchange interaction. In amorphous alloys only the distribution of the magnetic moments can be determined via the hyperfine field distribution. The standard fluctuation of the nearest neighbour exchange interaction,  $j$  around the reduced average value can be deduced from the temperature dependence of the standard width of the hyperfine field distribution [23]. The results are shown in Fig. 10 for a series of amorphous iron-rich alloys containing nonmagnetic components, including Fe-B [23], Fe-Zr [24],

Fe-Zr-B and Fe-Zr-Cu. It is remarkable that the  $j$  values obtained at the same Fe concentration but in alloys with rather different nonmagnetic elements are on the same curve.

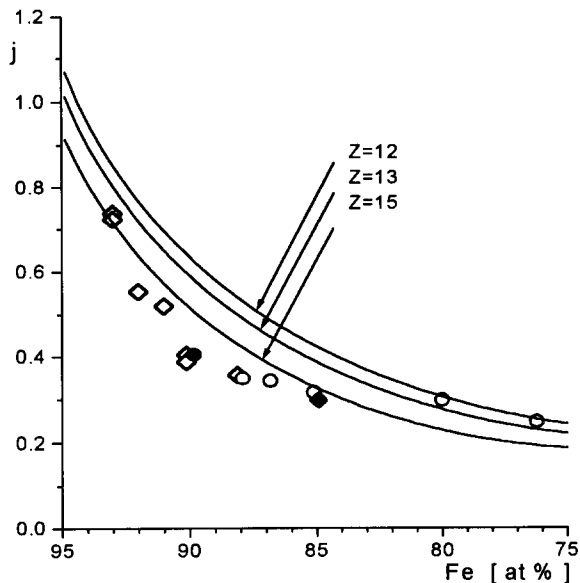


Fig. 10 The standard fluctuation of the nearest neighbour exchange interaction,  $j$  around the reduced average value as a function of iron composition for different amorphous alloys: Fe-Zr (diamonds), Fe-B (circles),  $\text{Fe}_{90}\text{Zr}_5\text{B}_5$  (filled circle) and  $\text{Fe}_{85}\text{Zr}_{10}\text{B}_5$  (filled diamond), respectively. The continuous curves are calculated in the simple model explained in the text.

The magnetic moment of iron strongly depends on its atomic volume: it is decreasing with decreasing volume and the magnetic coupling changes from ferromagnetic to antiferromagnetic [19]. The Fe atoms surrounded exclusively by Fe neighbours have a dominant influence to the anomalous magnetic properties of iron-rich Fe-Zr alloys [25]. These iron atoms are compressed and their magnetic moment is about  $1 \mu_B$ . The assumption that they are weakly coupled to the rest of the Fe magnetic moments reproduces quite well the observed trend in the reduced fluctuation of the exchange interaction of Fig. 10. Random distribution of the nonmagnetic atoms was assumed in the calculation using only two different Fe sites: single ferromagnetic coupling between iron atoms with nonmagnetic nearest neighbours and no magnetic coupling at all for iron atoms surrounded by other Fe atoms only. The results of this very simple model calculation are reproduced in Fig. 10 for different possible coordination numbers,  $Z$ .

In the proposed model the disappearance of the ferromagnetic state with increasing Fe concentration in these amorphous alloys is related to a bond percolation

problem: the compressed, low moment Fe atoms are decoupled from the ferromagnetic matrix. Their number is increasing with the decreasing nonmagnetic atom concentration and at around 7 at.% content it reaches a percolation threshold: the infinite ferromagnetic percolation cluster will cease to exist and the system undergoes a freezing transition, it becomes a spin glass. In the vicinity of the transition temperatures ( $T_C$  and  $T_f$ ) composition dependent Mössbauer investigation in small magnetic fields clearly shows the progressive transition from the apparent ferromagnetic behaviour into the spin glass state [26].

#### IV. SUMMARY

The anomalous magnetic properties of iron-rich amorphous alloys were studied via magnetization and high field Mössbauer measurements. These systems show the absence of magnetic saturation in large applied fields, the ferromagnetic Curie temperature decreases with increasing iron concentration. At the highest available iron concentration the ferromagnetic order breaks down resulting in a spin glass-like state which is extremely sensitive to impurities (e.g. H) and to the applied field.

Increasing amount of antiferromagnetic coupling between the iron moments due to their decreasing interatomic distances used to be the common explanation of the observed anomalies. An obvious consequence of this assumption is the appearance of the spin glass, re-entrant spin glass state, the presence of antiferromagnetically aligned Fe moments and consequently a noncollinear, canted spin structure. The absence of saturation, the very large high field susceptibility directly follows then from the collapsing of the noncollinear magnetic moment arrangement.

In systems which do not show spin freezing phenomena (soft ferromagnets, fine ferromagnetic particles, granular structures) the explanation for the absence of saturation used to be the assumption of the existence of strong local anisotropies due to the amorphous structure or surface states.

Our results fundamentally modify this picture. The absence of magnetic saturation for large applied fields has two important sources. One of them is the generally neglected contribution of shape anisotropy. This is always present when the shape of the investigated sample is not a perfect sphere or flat plane. It occurs, when surface irregularities cause the local orientation of the surface to bend from the direction parallel or perpendicular to the applied field. The ideal shape cannot be achieved in the case of melt-quenched ribbons or in granular systems which explains that magnetic saturation can not be achieved in fields significantly higher than the demagnetization field even in the absence of strong local anisotropy. The observed magnitude of the deviation from the behaviour theoretically expected for the ideal sample shape is

somewhat surprising. In this case saturation is not observed due to the misalignment between the moment of the collinear magnetic structure and the external field.

Recently complicated magnetization processes are observed in some few monolayer thick multilayer systems. The phenomenological description assumes the existence of biquadratic exchange coupling between the layers [27]. According to theoretical calculations the possible origin of this interaction is spatial fluctuations, surface roughness or loose spins due to intermixing of the layers. However, the calculated interaction strengths are larger (at least by one order of magnitude) than the experimental values. The effect of shape anisotropy discussed here for macroscopic samples may also be relevant in the case of the microscopic irregularities of few atom thick multilayers.

A second, not necessarily different source causes that normal ferromagnetic saturation is not observed for alloys showing spin freezing phenomena. We found that the magnetic structure is already collinear in such applied fields where the magnetic saturation is not yet reached. These magnetic fields are much lower than the values expected on the base of the freezing temperature characteristic of the interaction strength. In this collinear field range the field dependence of the magnitude of the individual Fe magnetic moments (measured locally via the Mössbauer hyperfine fields) was in good agreement with that of the bulk magnetization. This observation rules out the assumption of antiferromagnetically aligned Fe moments as the origin of the extremely large high field susceptibility. The temperature dependence of the magnetic moments measured via the iron hyperfine field distribution does not support the presence of a substantial antiferromagnetic exchange interaction. It may be explained, however, by assuming the decoupling of the moment of iron atoms with iron nearest neighbours only, from the moments of its surrounding. The existence of the decoupling is attributed to the well-known anomalous volume dependence of the magnetic properties of iron.

This decoupling scheme emerges as the mechanism of the spin freezing phenomena instead of the frustrated exchange interaction model. It is a bond percolation problem: iron atoms with only iron nearest neighbours are decoupled from the matrix. Their number is increasing with increasing iron concentration, thus the decoupling (or weak coupling) results in magnetically separated regions. When the percolation threshold is achieved the infinite ferromagnetic cluster ceases to exist and freezing of the direction of the collinear magnetic moments of the separated regions takes place. In these systems magnetic clustering due to statistical reason occurs without the sign of any chemical clustering. The shape anisotropy of the irregular separated regions may play a significant role in the freezing. Little is known of the effect of shape anisotropy of an infinite percolation cluster with fractal structure. It may explain the contradictory magnetic properties of spin glasses: fast increase of the

magnetization in low fields, slow approach to saturation in high applied fields.

The infinite ferromagnetic percolation cluster will coexist with magnetically separated but collinearly correlated magnetic regions which have a rather broad relaxation time distribution. This may explain both the very large high field susceptibility values characteristic of spin glasses and re-entrant spin glasses. The large amount of induced magnetic moments at higher temperatures (as indicated by the non-conventional Mössbauer magnetization curves for alloys at compositions not showing the spin freezing characteristics) may have the same origin.

According to the present results spin glasses may be termed as mesoscopic ferromagnets with complicated fractal structure: the characteristic size of the structure is comparable to the range of the characteristic exchange interaction. The magnetic properties of granular systems are similar when the effect of irregular shape is dominant and differ when effects due to the infinite size come into play.

Acknowledgements – We gratefully acknowledge helpful discussions with J. Balogh, D. Kaptás and L. F. Kiss and the use of their results prior to publication. This work was supported by the Hungarian National Research Fund OTKA T4464 and T17456.

## REFERENCES

- [1] e.g. J. A. Mydosh, Spin glasses: an experimental introduction, Taylor&Francis, London, Washington, DC, 1993.
- [2] I. A. Campbell and S. Senoussi, *Phil. Mag.* **65B**, 1267 (1992).
- [3] J. J. Smit, G. J. Nieuwenhuys and L. J. de Jongh, *Solid St. Commun.* **32**, 233 (1979).
- [4] H. Hiroyoshi and K. Fukamichi, in *High Field Magnetism*, edited by M. Date (North-Holland, Amsterdam, 1983), p. 113.
- [5] J. Lauer and W. Keune, *Phys. Rev. Letters* **48**, 1850 (1982).
- [6] S. Lange, M. M. Abd-Elmeguid and H. Micklitz, *Phys. Rev.* **B41**, 6907 (1990).
- [7] M. M. Abd-Elmeguid, H. Micklitz, R. A. Brand and W. Keune, *Phys. Rev.* **B33**, 7833 (1986).
- [8] D. Wiarda and D. H. Ryan, *J. Appl. Phys.* **76**, 6377 (1994).
- [9] T. E. Cranshaw, *J. Appl. Phys.* **40**, 1481 (1969).
- [10] R. A. Cowley, C. Patterson, N. Cowlam, P. K. Ivison, J. Martinez and L. D. Cussen, *J. Phys.: Condens. Matter* **3**, 9521 (1991).
- [11] Q. A. Pankhurst and M. R. J. Gibbs, *J. Phys.: Condens. Matter* **5**, 3275 (1993).
- [12] S. J. Harker and R. J. Pollard, *J. Phys.: Condens. Matter* **1**, 8269 (1989).
- [13] C. D. Graham, Jr and M. R. J. Gibbs, *IEEE Trans. Magn.* **29**, 3457 (1993).

- [14] T. Ono, N. Hosoito and T. Shinjo, *J. Phys. Soc. Japan* **63**, 2874 (1994).
- [15] M. W. Grinstaff, M. B. Salamon and K. S. Suslick, *Phys. Rev.* **B48**, 269 (1993).
- [16] L. F. Kiss and N. Hegman, *J. Magn. Magn. Mat.* **140-144**, 293 (1995).
- [17] J. L. Tholence, *Physica* **B126**, 157 (1984); J. L. Dormann, L. Bessais and D. Fiorani, *J. Phys. C: Solid State Phys.* **21**, 2015 (1988).
- [18] I. Vincze, D. Kaptás, T. Kemény, L. F. Kiss, and J. Balogh, *Phys. Rev. Letters* **73**, 496 (1994).
- [19] Y. Kakehashi and M. Yu, *Phys. Rev.* **50**, 6189 (1994); R. Lorenz and J. Hafner, *J. Magn. Magn. Mat.* **139**, 209 (1995).
- [20] H. G. Wagner, U. Gonser and A. Schertz, in *Rapidly Quenched Metals III*, Vol. 2, ed. B. Cantor (London: Metal Society), 1978, p.333.
- [21] S. Foner, A. J. Freeman, N. A. Blum, R. B. Frankel, E. J. McNiff, Jr. and H. C. Pradhaude, *Phys. Rev.* **181**, 863 (1969).
- [22] e.g. F. Varret, A. Hamzic and I. A. Campbell, *Phys. Rev.* **B26**, 5285 (1982); M. Ghafari, R. K. Day, J. B. Dunlop and A. C. McGrath, *J. Magn. Magn. Mat.* **104-107**, 1668 (1992).
- [23] I. Vincze, J. Balogh, Z. Fóris, D. Kaptás and T. Kemény, *Solid St. Commun.* **77**, 757 (1991).
- [24] D. Kaptás, T. Kemény, J. Balogh, L. F. Kiss, L. Gránásy and I. Vincze, *Hyperfine Int.* **94**, 1861 (1994).
- [25] D. Kaptás, T. Kemény, L. F. Kiss, L. Gránásy, J. Balogh and I. Vincze, *J. of Non-Cryst. Solids* **156-158**, 336 (1993).
- [26] D. Kaptás, T. Kemény, L. F. Kiss, J. Balogh, L. Gránásy and I. Vincze, *Phys. Rev.* **B46**, 6600 (1992).
- [27] M. Schäfer, Q. Leng, R. Schreiber, K. Takanashi, P. Grünberg and W. Zinn, *Mat. Sci. Eng.* **B31**, 17 (1995); J. C. Slonczewski, *Phys. Rev. Letters* **67**, 3172 (1991); *J. Appl. Phys.* **73**, 5957 (1993).